The Kinetic and Mechanism of Crystallization of $MgGeO_3$ in $65GeO_2$-15PbO-$10MgF_2$-10MgO Glass System

M. Nouri[1], P. Alizadeh[1] and M. Tavoosi[*2]

* *ma.tavoosi@gmail.com*

Received: April 2017 Accepted: August 2017

[1] Department of Materials Engineering, Tarbiat Modares University, Tehran, Iran.
[2] Department of Materials Engineering, Malek-Ashtar University of Technology, Tehran, Iran.
DOI: 10.22068/ijmse.14.3.64

Abstract: *In this study, the crystallization behavior of a $65GeO_2$-15PbO-$10MgF_2$-10MgOglass (prepared by the conventional melt quenching technique) has been investigated. The microstructure and crystallization behaviors of this glass were characterized using X-ray diffraction (XRD), scanning electron microscopy (SEM), non-isothermal differential thermal analysis (DTA) and Fourier transform infrared spectroscopy (FTIR).The results demonstrated that a fully glassy phase can successfully be prepared by the conventional melt quenching technique exhibiting one-stage crystallization on heating, i.e., the glassy phase transforms into crystalline $MgGeO_3$ and Pb_5GeO_7 phases. The activation energy for the crystallization, evaluated from the Kissinger equation, was approximately 202±5 kJ/mole using the peak temperature of the exothermic reaction. The Avrami exponent or reaction order,n, indicates the nucleation rate in this glass to increase with time and the crystallization to be governed by a three-dimensional interface-controlled growth.*

Keywords: *Lead-Germanate Glass, Crystallization, Nucleation, Growth, Kinetic.*

1. INTRODUCTION

The middle infrared range, at the wavelength range of 3-5 μm, is the most important atmospheric transmission windows and transparent materials in this range are especially important for optical applications[1]. It is well known that, transparent materials for optical applications must provide maximum transmission and withstand the thermal shock and abrasion. These materials must be isotropic and easily fabricated at low costs. However, an ideal window satisfying all the requirements does not exist and selection of an IR window is often based on compromises instead of choices [2-4].

Among window materials for IR applications (eg; ZnS, sapphire, AlON and some glasses), germanate glasses have been of interest due to the excellent combination of IR transparency, chemical durability, and availability in desired shape and size [2]. However, low mechanical properties (strength and elastic modulus) are the major limitation of these glasses used in high speed airborne missiles.

One of reasonable approaches to combat the above drawback is to convert germanate glasses to germanate glass-ceramics, via controlled crystallization process. For instance, Bayya et al. [5] confirmed that the ceramization of BaO-Ga_2O_3-GeO_2 glass results in a significant improvement of the physical and mechanical properties of the base glass. Tang et al. [6] also showed that the mechanical and thermal properties of BaO-GeO_2 glasses can be significantly enhanced during controlled crystallization which also has no effect on transparency.

Thus, the crystallization behavior evolutions of the $65GeO_2$-15PbO-$10MgF_2$-10MgO glass were the aim of this study. In this regard, the desired glass was prepared by using conventional melt quenching technique and the structural and phase changes, during melt quenching and annealing processes, were evaluated. Moreover, the crystallization kinetics of this glass were analyzed and value of the crystallization activation energy and the Avrami exponent were established.

2. EXPERIMENTAL PROCEDURE

High purity GeO_2 (99.9% purity), PbO

[DOI: 10.22068/ijmse.14.3.64]

(99.99% purity), MgO (99.99% purity) and MgF_2 (99.99% purity) were used as raw materials. A mixture of initial precursor with a nominal composition of $65GeO_2$-15PbO-10MgO-$10MgF_2$ was melted in an alumina crucible at 1400ºC for 15minutes. The melt was poured on two stainless steel plates and pressed to form disks of 2 mm thickness. In the present experiments, yellowish transparent glass, without any bubbles and inclusions, was easily formed on rapid quenching of the melt. Heat treatment procedure had been done at ambient atmosphere in temperatures range of 625 to 820ºC for different periods of time.

XRD technique, using a diffractometer with Cu K_α radiation (λ= 0.15406 nm; 40 kV; Philips PW3710) was used to follow the structural changes of the specimens (step size: 0.05º; time per step: 1s). Structural characterizations of samples were studied using a field emission scanning electron microscopy (VEGA-TESCAN-XMU) at an accelerating voltage of 20kV.A differential thermal analysis,using a Reometric STA 1500 differential thermal analyzer, was also used to study the thermal stability of the sample. Samples were placed in Al_2O_3 pans and heated in a dynamic argon atmosphere up to 1000 °C at different heating rates of 10 to 25 °C/min. Optical properties of samples were also measured using a Bruker Tensor 27 FTIR spectrometer.

3. RESULTS AND DISCUSSION

The melting point of GeO_2, MgO, MgF_2 and PbO are 1120, 2825, 888 and 1263ºC, respectively. The relative low melting point of PbO suggests that short heating time should be applied to GeO_2-PbO-MgO-MgF_2 system. For this reason, melting interval times of 15-30 minutes seems to be an appropriate duration in order to avoid the evaporation of PbO and destroying the stoichiometry. Consequently, initial precursor with a nominal composition of $65GeO_2$-15PbO-10MgO-$10MgF_2$ was melted at 1400ºC for 30 minutes and then was quenched between two stainless steel plates. Obtained XRD pattern of the sample is shown in Fig. 1. The broad diffuse scattering at low angles in this figure confirms a long-range structural disorder characteristic of an amorphous network.

The infrared absorption spectra of prepared glass (Fig. 2) shows broad absorption bands which is in agreement with the amorphous nature of the samples suggested by the X-ray diffraction pattern. The spectra in Fig. 2 is characterized by two wide absorption bands around 500-700 and 700-1100 cm^{-1}. Absorption at 585 cm^{-1} indicates

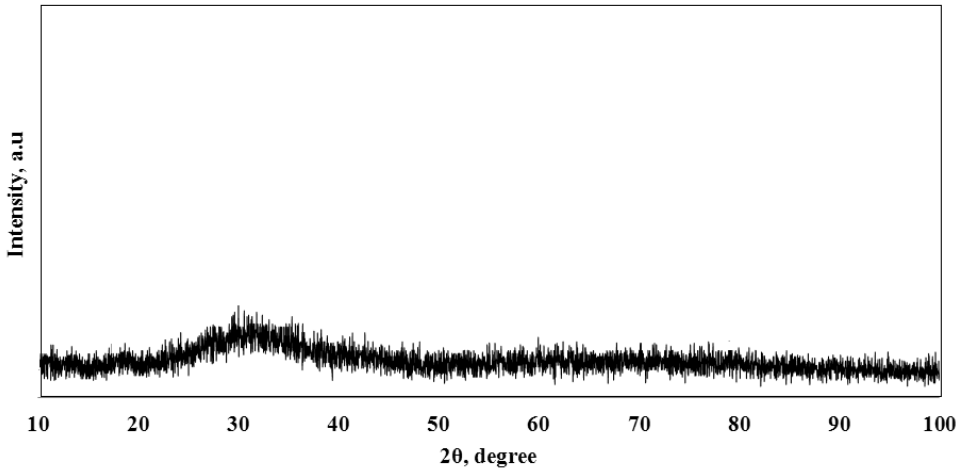

Fig.1. The XRD pattern of prepared $65GeO_2$-15PbO-10MgO-$10MgF_2$ glass.

[DOI: 10.22068/ijmse.14.3.64]

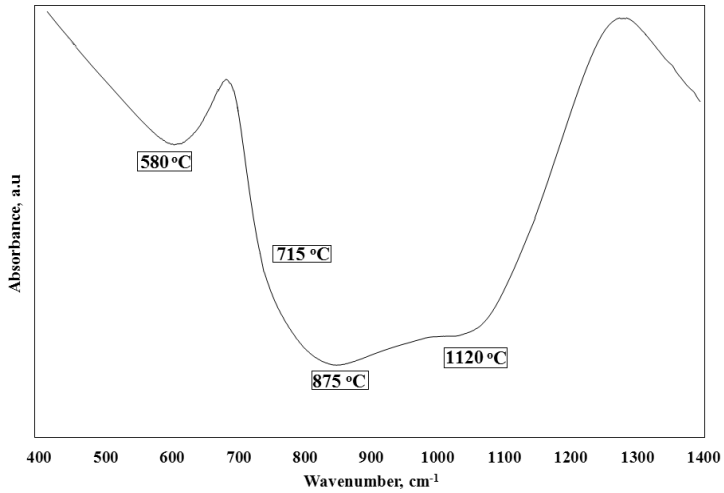

Fig. 2. The FTIR spectra of prepared $65GeO_2$_15PbO_10MgO_10MgF_2 glass.

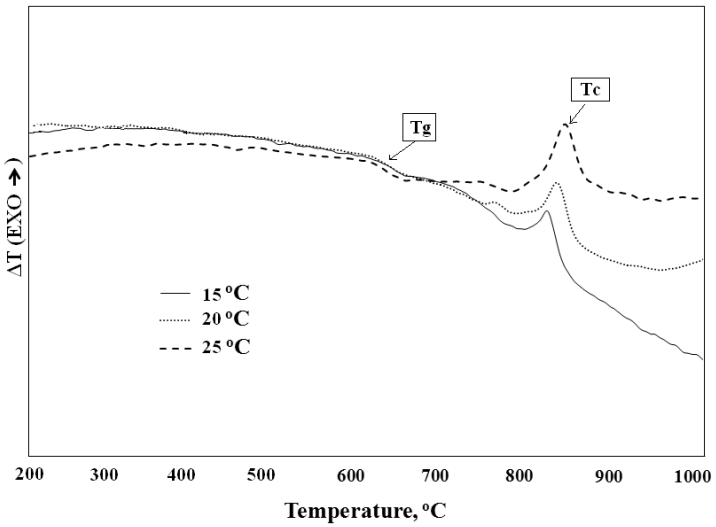

Fig. 3. The DSC heating traces of as-quenched $65GeO_2$_15PbO_10MgO_10MgF_2 sample at different heating rates (Tg=glass transition temperature, Ts= softening temperature and Tc=crystallization temperature).

bending and symmetric stretching vibration of the Ge-O-Ge of GeO_4 tetrahedral unit (with the Ge-O bonds of 1.739±0.002 A°) [7]. The band at wave number of 700-1100 cm^{-1} can be divided to three peaks at 715, 875 and 1020 cm^{-1}. The first peak is related to stretching vibration mode of the Ge-O-Ge bond in GeO_6 octahedral units of germanium oxide (where four Ge-O bonds are of 1.827 A°, while the other two are of 1.902 A° [7]), the second is related to anti-symmetric stretching vibration mode of the Ge-O-Ge bond in GeO_4 tetrahedral units [8] and the third is related to anti-symmetric bending vibration of Pb-O-Pb bond in [PbOn] unites. Based on these FTIR spectra (Fig. 2), the Ge^{4+} cations are incorporated in the studied GeO_2_PbO glass system as GeO_4 and GeO_6 units. As maintained by Prasad et al. [8], PbO can participate in the glass network with PbO_4 structural units. In this structure, each lead ion is linked to four oxygen atoms by covalence

[DOI: 10.22068/ijmse.14.3.64]

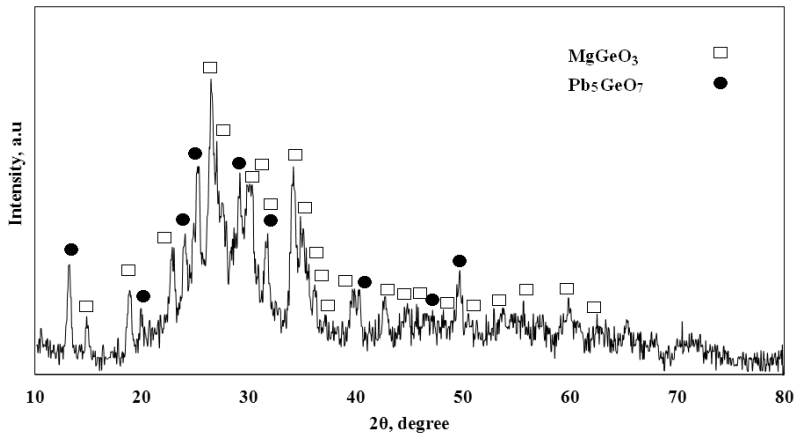

Fig. 4. The XRD pattern of as-quenched $65GeO_2$_15PbO_10MgO_$10MgF_2$ sample after annealing at 800 °C for 60 minutes.

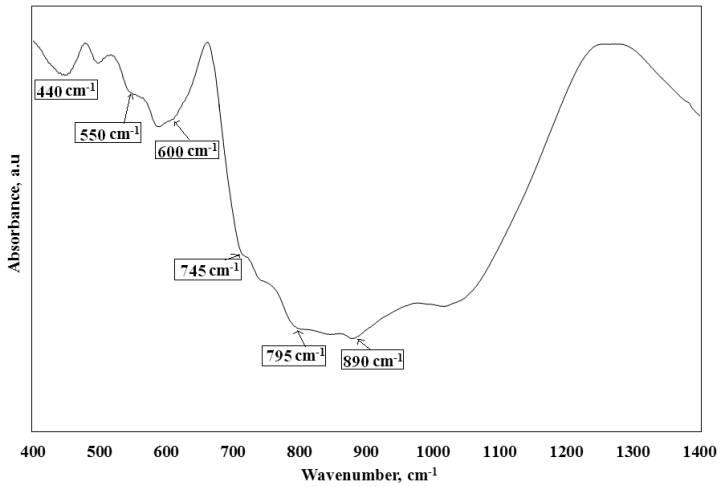

Fig. 5. The FTIR spectra of as-quenched $65GeO_2$_15PbO_10MgO_$10MgF_2$ sample after annealing at 800 °C for 60 minutes.

bonding.

To study the crystallization behavior of prepared glass and define the appropriate annealing temperature in this sample, DSC analyses were carried out. The DSC heating traces of as-quenched $65GeO_2$_15PbO_10MgO_$10MgF_2$ sample at different heating rates are presented in Fig. 3. As seen, only one exothermic peak at temperature range of 750-850ºC appears in DSC curves. To analyze the crystallization process responsible for this exothermic peak, the sample was annealed at 800ºC for 60 minutes. The XRD pattern, FTIR spectrum and SEM micrographs of annealed sample are presented in Figs. 4 & 6, respectively. As seen, this sample mainly consists of $MgGeO_3$ and Pb_5GeO_7 phases. The FTIR spectrum of this sample which is presented in Fig. 5, also confirm this finding. In fact, the additional absorption bands in this spectrum (at 440, 550, 600, 745, 795 and 890 cm^{-1}) can be related to crystalline magnesium-germanate phase [9]. Moreover, according to SEM findings shown in Fig. 6, the microstructure of the sample consists of $MgGeO_3$ precipitates (with Blood River like structure) which are dispersed in Pb_5GeO_7 matrix. By paying attention

[DOI: 10.22068/ijmse.14.3.64]

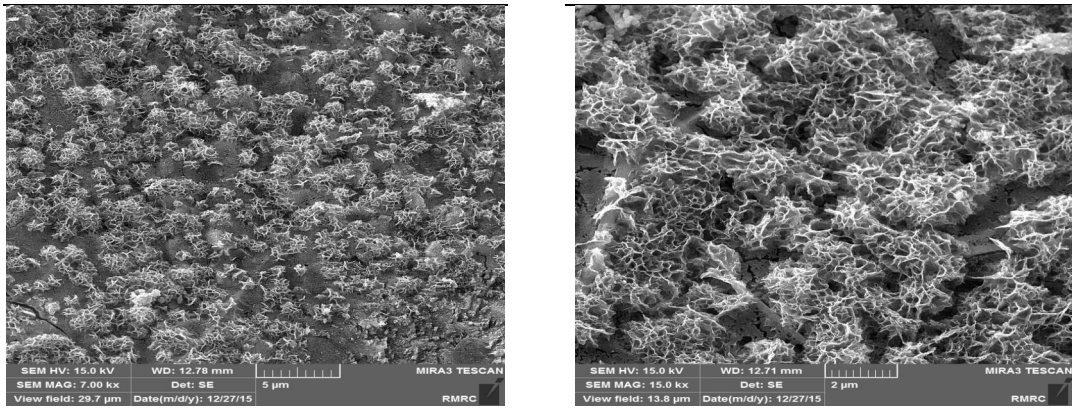

(a) (b)

Fig. 6. The SEM micrographs of as-quenched $65GeO_2$-$15PbO$-$10MgO$-$10MgF_2$ sample after annealing at 800 °C for 60 minutes, a) complex overview; b) more detailed view.

to these results, the exothermic peak in Fig. 3 can be attributed to precipitation of $MgGeO_3$ and Pb_5GeO_7 from the amorphous matrix.

The crystallization of amorphous phases is a diffusional process and is known to generally proceed by nucleation and growth processes. This process starts at temperatures in which atomic diffusion starts and the rate of crystallization increases with increasing temperature. Crystallization studies of amorphous materials at lower temperature (under crystallization temperature) are interesting from many points of view. The results of such studies are helpful in understanding the mechanism and kinetics of phase transformation into the equilibrium conditions. They also allow us to evaluate the thermal stability of the amorphous state [10].

The XRD patterns of samples annealed at 700, 760 and 820ºC for 60 minare shown in Fig. 7. It is important to note that, before annealing treatment, the prepared samples were nucleated at 625ºC for 5 h (Tnucl.=(TS+Tg)/2). As seen, the XRD pattern of as-nucleated sampleonly consists of two narrow peaks corresponding to $MgGeO_3$ phase which is located on amorphous halo. By annealing the sample at 700ºC, the intensity of $MgGeO_3$ peaks increase and several additionalpeaks ofthis phase appear in XRD pattern. In fact, increasing the annealing temperature,beyond 760ºC, leads to the precipitation of Pb_5GeO_7 phase from remaining amorphous matrix. Therefore, the structural changes during annealing of $65GeO_2$-$15PbO$-$10MgO$-$10MgF_2$ glass can be written as: Amorphous→Amorphous+$MgGeO_3$→ Pb_5GeO_7+$MgGeO_3$. This result illustrates that, the crystallization mechanism in this glassy system is primary crystallization.

The crystallization kinetics of amorphous materials can be described by three parameters, namely, the crystallization activation energy, the Avrami exponent and the frequency factor. In calorimetric measurements, non-isothermal methods can be used to calculate these parameters. The theoretical basis for interpreting thermal analysis data for crystallization is provided by the classical Johnson-Mehl-Avrami (JMA) model. In this model, the crystallized volume fraction (α) can be expressed as a function of time according to the following relation [11-13]:

$$\alpha(t)=1-\exp[-Kt^n] \quad (1)$$

[DOI: 10.22068/ijmse.14.3.64]

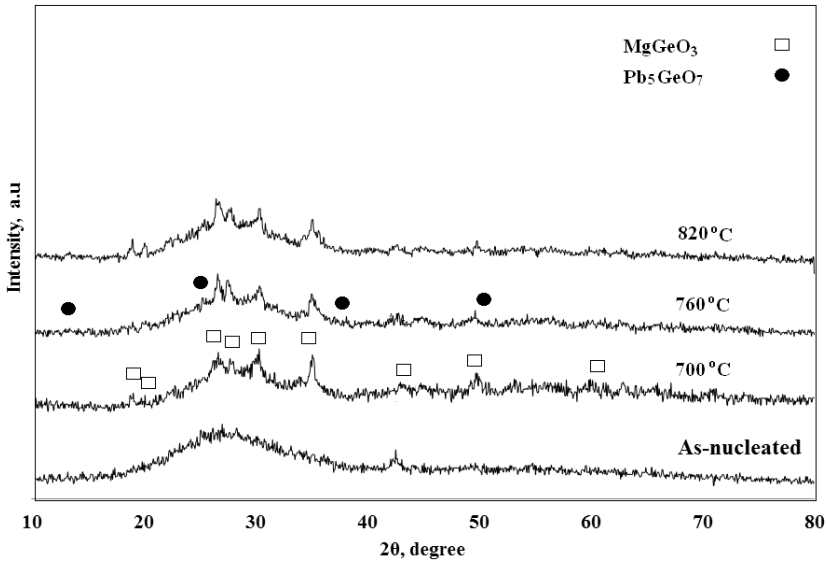

Fig. 7. The XRD patterns of $65GeO_2$-15PbO-10MgO-$10MgF_2$ glass after nucleation (at 625 ºC for 5 h) and annealing at 700, 760 and 820 ºC for 60 minutes.

where K is defined as the effective overall reaction rate constant and n is the Avrami exponent. The constant K usually has Arrhenius temperature dependence as follows:

$$K=K_0 \exp((-E)/RT) \quad (2)$$

where K_o is the frequency factor, T is temperature, and E is the activation energy describing the overall crystallization process. The effective activation energy of the crystallization can be estimated using Kissinger's equation [14] using the non-isothermal DTA measurements as follows:

$$\ln(\beta/(T_P^2)) = (E/(RT_P)) + constant \quad (3)$$

where T_P is the highest temperature of the exothermic peak, β is the heating rate, R is the gas constant, and E is the effective activation energy of the crystallization. Kissinger's plot $\ln(\beta/T_P^2)$ versus 1/T results in approximately straight lines. It is important to note that, the mathematical derivation of Kissinger's model is only valid when the glass to crystal reaction is assumed to be first order [15]. This assumption is not valid for the many case of crystallization phenomenon in glasses.Based on the slope of Kissinger's plots of $65GeO_2$-15PbO-10MgO-$10MgF_2$ glass (Fig. 8), the effective activation energy of the crystallizationwas estimated about 202±5 kJ/mol.

The area under the DTA curve is directly proportional to the total amount of crystallized samples. The volume fraction of crystallized section of the samples, α, as a function of temperature, T, was obtained from the DTA curves (Fig. 3). It is important to note that before each study; the base line of DTA curves was removed using the NETZSCH software. The crystallized volume fraction,α, at any temperature T is given as:

$$\alpha = (A_T/A) \quad (4)$$

where A is the total area of the exothermic peak (between the temperature where the crystallization begins, T_i, and the temperature where the crystallization is completed, T_f) and AT is the area between the initial temperature and any temperature T (between T_i and T_f). The plots of α versus T at different heating rates are shown in Fig. 9. As seen, the shapes of these plots are typical sigmoidal shapes, which appear

[DOI: 10.22068/ijmse.14.3.64]

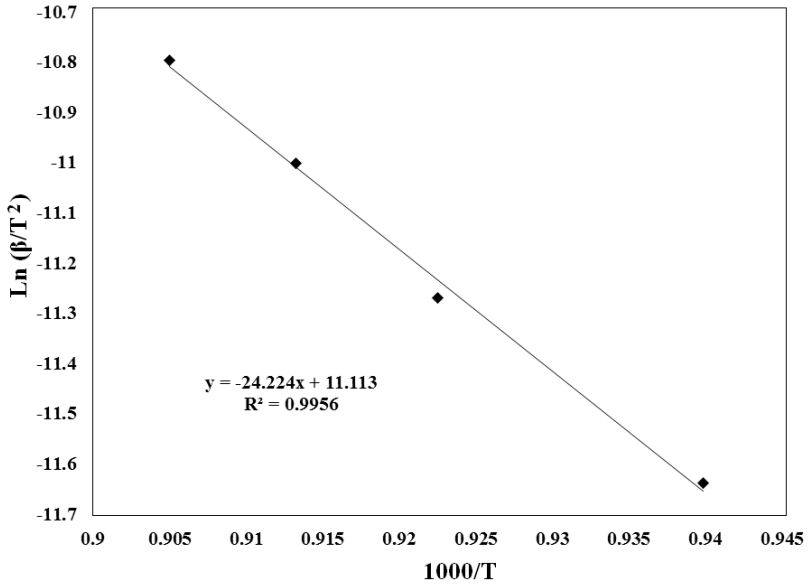

Fig. 8. The Kissinger's plot of $\ln(\beta/(T_P^2))$ versus 1000/T for crystallization of $65GeO_2$_15PbO_10MgO_10MgF_2 glass.

frequently in the literature [15-17]. The sigmoidal plots exhibit bulk crystallization and exclude the chance of surface crystallization [17].

The local activation energy of the crystallization, which changes with the crystallization fraction, can be determined using the Flynn-Wall-Ozawa method [18, 19]:

$$log\beta = log\frac{AE(\alpha)}{Rg(\alpha)} - 0.457\frac{E(\alpha)}{RT} - 2.315 \qquad (5)$$

where A is the pre-exponential factor, E(α) is the local activation energy of crystallization, and g(α) is a function determined by the crystallization fraction. In fact, a plot of log β versus 1000/T for the given values of the crystallization fraction gives the local activation energy of the crystallization. This method is employed to estimate the local activation energy of $65GeO_2$_15PbO_10MgO_10MgF_2 glass by analyzing the data in Fig. 9, and the final results are shown in Fig. 10. It can be seen that the local activation energy increases slightly with the progress of crystallization. This indicates that the crystallization process becomes more difficult as the crystallization fraction increases.

The crystallization kinetics can be determined using the DTA and fitting the data with the Johnson-Mehl-Avrami (JMA) model as noted by Ozawa [20]:

$$\ln[-\ln(1-\alpha)] = -n\ln(\beta) + \ln X(T) \qquad (6)$$

where n is the Avrami exponent. The following formula was obtained after the transformation of Eq. (6) at a constant temperature T:

$$\left.\frac{d\{ln[-ln(1-\alpha)]\}}{dln\beta}\right|_T = -n \qquad (7)$$

The Avrami exponent, n, were determined from the ln[-ln(1-α)] versus lnβ plot. As can be seen from Fig. 11, the Avrami exponent is in the range of $4.0<n<4.5$ and decreases with increasing temperature. The Avrami exponent provides detailed information of the nucleation and growth mechanisms. Ranganathan and Heimendahl [21] suggested that this exponent can be expressed as:

$$n = a + bc \qquad (8)$$

where a is the nucleation index, which can range

[DOI: 10.22068/ijmse.14.3.64]

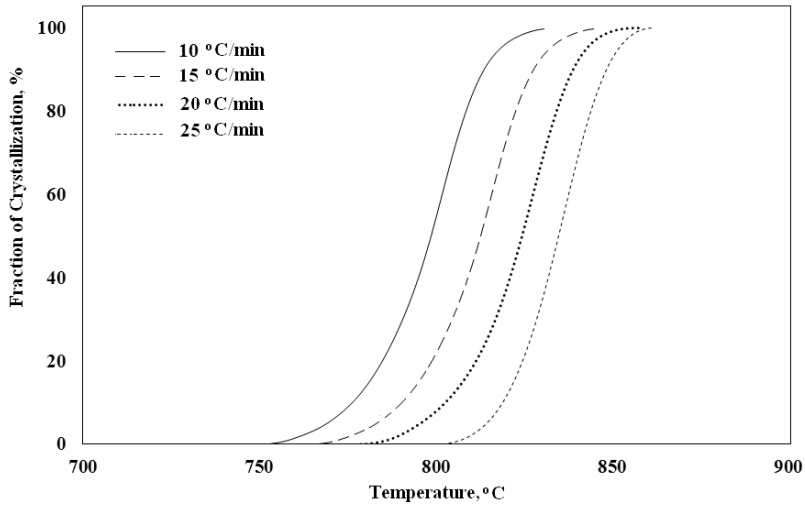

Fig. 9. Relationship between the crystallization fraction (α) and temperature (T) in the $65GeO_2$_15PbO_10MgO_$10MgF_2$ glass.

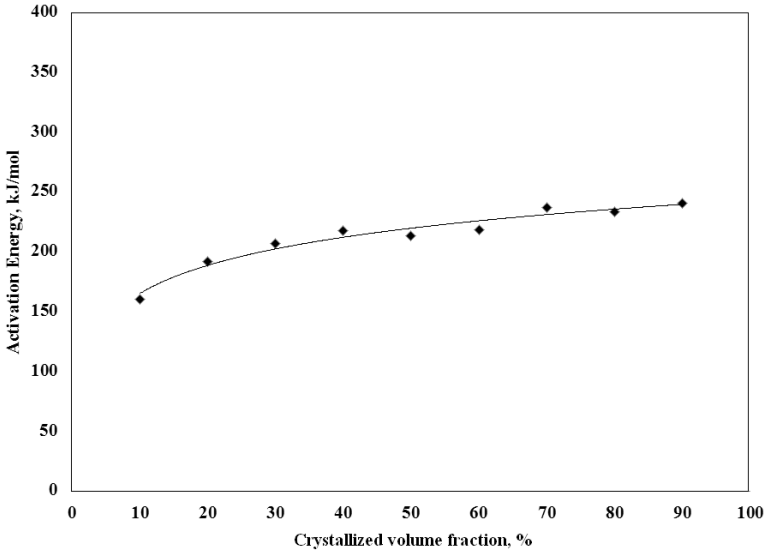

Fig. 10. Local crystallization activation energies versus the crystallization fraction in the $65GeO_2$_15PbO_10MgO_$10MgF_2$ glass.

from 0 to 1 (a=0 for a nucleation rate of zero, 0<a<1 for a nucleation rate decreasing with time, a=1 for a constant nucleation rate, and a>1 for an increasing nucleation rate),b is the dimension of the growth (with values 1, 2 or 3 for one, two, and three dimensional growth, respectively), and c is the growth index (c=1 for interface-controlled growth and c=0.5 for diffusion controlled growth). Based on above, the value of index a, b and c for crystallization of $65GeO_2$_15PbO_$10MgO$_$10MgF_2$ glass was estimated and the results were presented in Table 1. According to this table, the crystallization of the $65GeO_2$_15PbO_10MgO_$10MgF_2$ glass occurred with an increasing nucleation rate and was governed by a three-dimensional interface-controlled growth. In fact, the FE-SEM micrographs of annealed samples at 700°C for 30 minutes which are

[DOI: 10.22068/ijmse.14.3.64]

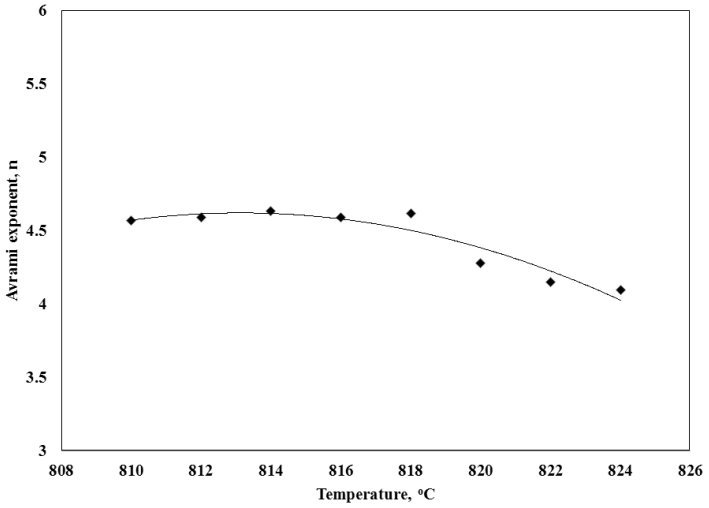

Fig. 11. Change of Avrami exponent with reference to the temperature.

Table 1. The value of index a, b and c (Ranganathan and Heimendahl indexs) for crystallization of $65GeO_2$-15PbO-10MgO-$10MgF_2$ glass.

Index	a	b	c
Estimated value	More than 1	3	1
Result	Increasing nucleation rate	Three dimensional growth	Interface-controlled growth

presented in Fig. 12 also confirm this finding.

It is important to note that, beside above-mentioned models which are commonly used in the glass community including this study, many other methods with different derivative have been also proposed by Piloyan- Borchardt [22, 23], Coats-Redfern [24], Šesták [25, 26] and Ligero et al. [27]. While all of thesemethods are based on the Johnson-Mehl-Avramitheory, they differ greatly in their assumption; and in some cases, they may lead to contradictory results. Therefore, controversy exists in using these models and ultimate care should be devoted.

Aside from the surface crystallization process, which has several issues to be solved for better kinetic understanding [28-30], the Avrami exponents which is valid for isothermal conditions extends to the transformation under non-isothermal conditions. In fact, this work imposes further complications of the theoretical interpretation of the kinetic results. The practical applicability of these models for the bulk crystallization process under non-isothermal conditions depends largely on the relationship between the independent kinetic processes of nucleation and growth. The temperature dependencies of nucleation and growth rates in non-isothermal treatment introduce further intricacies. It is generally accepted that the crystal growth from pre-existing nuclei without any secondary nucleation is successfully formalized by the JMA transformation kinetics even under non-isothermal conditions. On the other hand, the experimental resolution of the concurrent and consecutive processes of nucleation and growth in the same temperature

[DOI: 10.22068/ijmse.14.3.64]

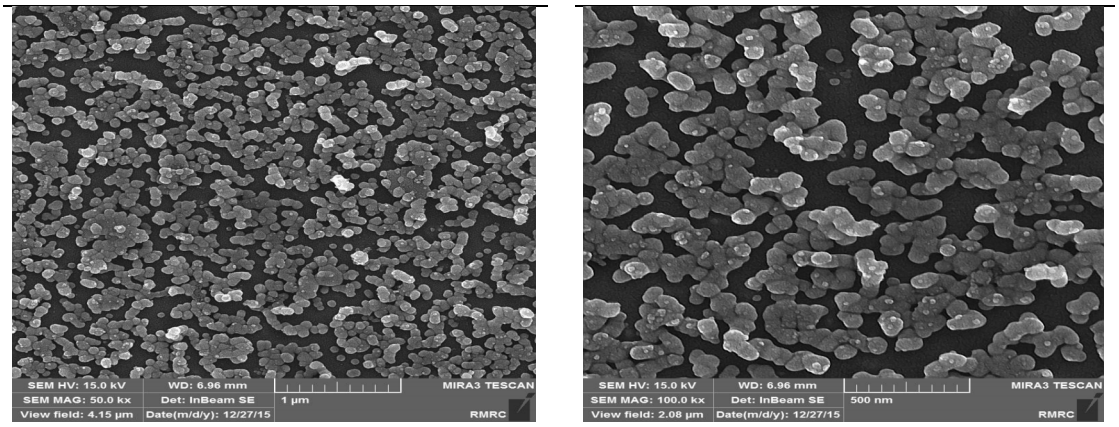

(a) (b)

Fig. 12. The SEM micrographs of as-quenched $65GeO_2$_15PbO_10MgO_10MgF_2 sample after annealing at 700 °C for 30 min, a) complex overview; b) more detailed view.

region is not always successfully described by the JMA transformation kinetics. Even for crystal growth from pre-existing nuclei, the direct application of the JMA transformation kinetics under non-isothermal condition leads to superficial kinetic results when the number of pre-existing nuclei changes depending on the thermal history within the temperature range for nucleation [31-33].

4. CONCLUSION

Based on our investigation of the crystallization kinetics of $65GeO_2$_15PbO_10MgO_10MgF_2 glass using a non-isothermal DTA analysis method, we summarize the primary results as follows. The fully glassy phase can successfully be prepared during conventional melt quenching technique in this system which exhibited one-stage crystallization on heating, i.e., the glassy phase transforms into crystalline $MgGeO_3$ and Pb_5GeO_7 phases. The activation energy for crystallization of this glass, evaluated from the Kissinger equation, was approximately 202±5 kJ/mole. The Avrami exponent ($4.0<n<4.5$) indicates the nucleation rate in this glass to increase with time and the crystallization to be governed by a three-dimensional interface-controlled growth.

REFERENCES

1. Harris, D. C., "SPIE Tutorial Texts Series", SPIE Optical Engineering Press, Bellingham, WA, 1992.
2. Higby, P. L., Aggarwal, I. D., "Properties of barium gallium germanate glasses", Journal of Non-Crystalline Solids 163, 1993, 303-308.
3. McMillan, P. W., "Glass-Ceramics, Academic Press", London, 1964.
4. Aoland, W. H. and Beall, G., "Glass Ceramic Technology", American Ceramic Society, 2002.
5. Bayya, S. S., Sanghera, J. S., Aggarwal, I. D., Wojcik, J. A., "Infrared Transparent Germanate Glass-Ceramics", Journal of the American Ceramic Society 85, 2002, 3114-3116.
6. Tang, B., Yang, Y., Fan, Y., Zhang, L., "Barium Gallogermanate Glass Ceramics for Infrared Applications", Journal of Materials Science and Technology, 2010, 26, 558-563.
7. Witkowska, A., Sikora, B., Trzebiatowski, K., Rybicki, J., "Germanate anomaly in heavy metal oxide glasses: an EXAFS analysis", Journal of Non-Crystalline Solids, 2006, 352, 4356-4361.
8. Prasad, P. S., Raghavaiah, B. V., Balaji Rao, R.,

[DOI: 10.22068/ijmse.14.3.64]

Laxmikanth, C., Veeraiah, N., "Dielectric dispersion in the PbO-MoO_3-B_2O_3 glass system", Solid State Communications, 2004, 132, 235-240.
9. Madon, M. and Price, G. D., "Infrared spectroscopy of the polymorphic series (enstatite, ilmenite, and perovskite) of $MgSiO_3$, $MgGeO_3$, and $MnGeO_3$", Journal of Geophysical Research: Solid Earth, 1989, 94,15, 687-15,701.
10. Ahmadi, S., Shahverdi, H. R., Saremi and S. S., "Kinetics of Nanocrystallization in $Fe_{55}Cr_{18}Mo_7B_{16}C_4$ bulk amorphous alloy", Iranian Journal of Materials Science and Engineering 7, 2010, 25-29.
11. Johnson, W. A. and Mehl, R. F., "Reaction kinetics in processes of nucleation and growth", Transactions of the American Institute of Mining and Metallurgical Engineers 135, 1939, 416-442.
12. Avrami, M., "Kinetics of Phase Change. I General Theory", The Journal of Chemical Physics 7, 1939, 1103-1132.
13. Avrami, M., "Kinetics of Phase Change. II Transformation Time Relations for Random Distribution of Nuclei", The Journal of Chemical Physics 8, 1940, 212-224.
14. H. E. Kissinger, Reaction kinetics in thermal analysis, Analytical Chemistry 29, 1957, 1702-1706.
15. Blainea, R. L., Kissinger, H. F., "Homer Kissinger and the Kissinger equation", Thermochimica Acta 540, 2012, 1-6.
16. Popescu, C., "Integral method to analyze the kinetics of heterogeneous reactions under non-isothermal conditions A variant on the Ozawa-Flynn-Wall method", Thermochimal Acta 285, 1996, 309-323.
17. Pratap, A., Lad, K. N., Rao, T. L. S., Majmudar, P. and Saxena, N. S. "Kinetics of crystallization of amorphous $Cu_{50}Ti_{50}$ alloy", Journal of Non-Crystalline Solids 345-346, 2004, 178-181.
18. Flynn, J. H., Wall, L. A., Quick, A., "Direct method for the determination of activation energy from thermogravimetric data", Polymer Letter, 4, 1966, 323–328.
19. Ozawa, T., "A new method of analyzing thermogravimetric data", Bulletin of the Chemical Society of Japan 38, 1965, 1881-1886.
20. Ozawa, T., "Kinetics of non-isothermal crystallization", Polymers 12, 1971, 150-158.
21. Ranganathan, S. and Heimendahl, M. V., "The three activation energies with isothermal transformations: applications to metallic glasses", Journal of Materials Science16, 1981, 2401-2404.
22. Piloyan, G. O., Ryabchikov, I. D. and Novikova, O. S., "Determination of activation energies of chemical reactions by differential thermal analysis", Nature 212, 1966, 1229-1302.
23. Borchardt, H. J., "Initial reaction rates from DTA", Journal of Inorganic and Nuclear Chemistry 12, 1960, 252-254.
24. Coats, A. W. and Redfern, J. P., "Kinetic parameters from thermogravimetric data", Nature, 201, 1964, 68-69.
25. Šesták, J., "Applicability of DTA to the study of crystallization kinetics of glasses", Physics and Chemistry of Glasses 15, 1974, 137-140.
26. Šesták, J., "On the applicability of the p(x)-function to the determination of reaction kinetics under non-isothermal conditions", Thermochimica Acta 3, 1971, 150-154.
27. Ligero, R. A., Vazques, J., Villares, P. and Jimenez-Garay, R., "A study of the crystallization kinetics of some Cu-As-Te glasses", Journal of Materials Science 26, 1991, 211-215.
28. Rezvani, M., "Effects of various nucleation agents on crystallization kinetic of OFLAS glass ceramics", Iranian Journal of Materials Science and Engineering 8, 2011, 41-49.
29. Ozawa, T., "Kinetics of growth from pre-existing surface nuclei", Journal of Thermal Analysis and Calorimetry 82, 2005, 687-690.
30. Henderson, D. W., "Thermal analysis of non-isothermal crystallization kinetics in glass forming liquids", Journal of Non-Crystalline Solids 30, 1979, 301-315.
31. Henderson, D. W., "Experimental analysis of non-isothermal transformations involving nucleation and growth, Journal of Thermal Analysis 15, 1979, 325-331.
32. Matusita, K., Sakka, S., "Kinetic study of the crystallization of glass by differential scanning calorimetry", Physics and Chemistry Glasses

[DOI: 10.22068/ijmse.14.3.64]

20, 1979, 81-84.

33. Yinnon, H. and Uhlmann, D. R., "Applications of thermoanalytical techniques to the study of crystallization kinetics in glass-forming liquids", part I: Theory, Journal of Non-Crystalline Solids 54, 1983, 253-275.

[DOI: 10.22068/ijmse.14.3.64]